

# Divergent Mechanistic Pathways for Copper(I) Hydrophosphination Catalysis: Understanding that Allows for Diastereoselective Hydrophosphination of a Tri-substituted Styrene

Steven G. Dannenberg, Dennis M. Seth Jr., Emma J. Finfer, and Rory Waterman

Department of Chemistry, University of Vermont, Burlington, Vermont 05405-0125, USA

**KEYWORDS:** *copper catalysis, photocatalysis, hydrophosphination, phosphido, phosphine, phosphorus*

**ABSTRACT:** Readily available and bench-stable  $\text{Cu}(\text{acac})_2$  (**1**) addresses many challenges in exploratory hydrophosphination catalysis. Mechanistic investigations were performed to answer questions that remain about the reactivity of **1**, the role of light in the catalysis, and to provide direction for further study. A divergent Hammett plot indicates differing mechanisms based on electron density at the alkene substrate. A radical process was eliminated based on trapping reactions and in-situ EPR experiments. Isotopic labeling experiments, a zwitterionic trapping experiment, stoichiometric model reactions, and catalytic reactions using proxy intermediates indicate that both conjugate addition and insertion-based mechanistic pathways occur with this system, depending on the unsaturated substrate. Computational analysis indicates that the lowest energy transition is a ligand-to-metal charge transfer (LMCT) from the phosphido ligand where the LUMO has significant Cu–P antibonding character, suggesting that a weakened Cu–P bond accelerates insertion under photocatalytic conditions. This hypothesis explains the greater activity of **1** compared to copper-catalyzed hydrophosphination reports and appears to be a general phenomenon for copper(I) catalysts. These results have been leveraged to achieve heretofore unknown catalytic hydrophosphination reactivity, namely the diastereoselective hydrophosphination of a tri-substituted styrene substrate.

## INTRODUCTION

Organophosphines are integral molecules in catalysis, synthetic chemistry, materials science, and more.<sup>1,2,3</sup> Metal-catalyzed hydrophosphination, the addition of a P–H bond across an unsaturated substrate, is one of the most promising, and atom-economical, P–C bond forming reactions.<sup>4–14</sup> Progress has been made in expanding the available catalysts, scope, and selectivity of hydrophosphination in recent years.<sup>15–36</sup> However, limitations remain that hamper the synthetic utility of hydrophosphination.<sup>7, 12</sup> Among the most notable limitations with known catalysts is that they often require special preparation and/or complex ancillary ligands and that most pre-catalysts are not air- and water-stable (i.e., not convenient). Known catalysts also have limitations in reactivity, often stymied by unactivated or highly substituted substrates, especially in intermolecular reactions.<sup>7, 12</sup>

As reported in 2020, commercially available and bench-stable  $\text{Cu}(\text{acac})_2$  (**1**) addresses many challenges in exploratory hydrophosphination catalysis.<sup>37</sup> Compound **1** is highly active, effective for a range of activated and unactivated alkenes and alkyne substrates, tolerates primary and secondary phosphines, does not require an ancillary ligand, and operates at ambient temperature under photolysis in either the UV or visible, though thermal conditions also provide reactivity. The ease of use of **1** and its activity with a broad range of substrates, make hydrophosphination available to the wider synthetic

community. In light of these positive features, further mechanistic investigation was warranted to answer questions about the reactivity of **1** with both activated and unactivated substrates as well as the role of light in the reaction. Such studies often provide a springboard for identifying new reactivity.<sup>8, 15</sup>

Prior study of **1** in photocatalytic hydrophosphination garnered some initial understanding, but that work was primarily focused on the activation of copper. In that report, it was demonstrated that **1** is reduced by the phosphine substrate to generate an active Cu(I)-phosphido intermediate, 2 equiv. of acetylacetone, and 0.5 equiv. of diphosphine.<sup>37</sup> Solution behavior of **1** under these conditions is consistent with  $[(\text{Ph}_2\text{PH})\text{CuPPh}_2]_n$ . The copper(I) compound  $[(\text{PPh}_3)\text{CuH}]_6$ ,<sup>37</sup> which is a precursor to  $(\text{PPh}_3)\text{CuPPh}_2$  upon treatment with  $\text{Ph}_2\text{PH}$ ,<sup>38</sup> was also an effective precatalyst. Prior study of copper compounds in hydrophosphination catalysis are consistent with these observations,<sup>16, 25, 26, 37, 39–43</sup> but the observation of successful hydrophosphination of unactivated alkenes with **1** is unique among that series and tied to photocatalytic conditions. That reactivity indicates that the operant mechanism of P–C bond formation is migratory insertion. A more thorough understanding of mechanism would inform a transition to a prefabricated copper(I) catalysts that may promote additional reactivity to address specific challenges in hydrophosphination catalysis.<sup>7, 12</sup>

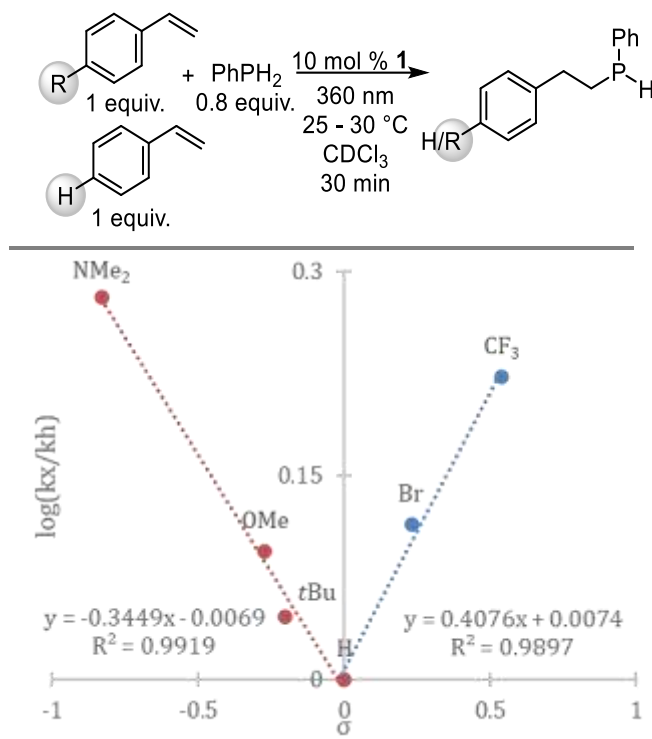
Herein, we report direct evidence of a catalytically active copper(I)–phosphido intermediate and that divergent mechanistic steps occur in the catalysis depending on the alkene substrate. Data in support of these mechanisms include a Hammett analysis, modified catalytic reactions with radical traps, a comparison of copper precursors, catalytic reactions of proxy intermediates, isotopic labeling experiments, a zwitterionic trapping experiment, and stoichiometric model reactions. Computational analysis provides key insight into photocatalysis demonstrating that the lowest energy transition, a ligand-to-metal charge transfer (LMCT), appears to weaken the Cu–P bond. This understanding allows for expansion of hydrophosphination with **1** to more difficult substrates, including the first example of a tri-substituted styrene. Additional primary phosphines and sterically hindered alkenes were also demonstrated as viable substrates, in recognition of the limitations of scope in hydrophosphination catalysis.<sup>7</sup> Throughout this study multiple light sources are demonstrated to be effective for this system and illustrate that commercially available bulbs are effective rather than specialty photoreactors, increasing the utility of this catalyst in exploratory reactions.

## RESULTS AND DISCUSSION

### Hammett analysis

As an initial probe of mechanism, a Hammett analysis was performed using substituted styrene substrates.<sup>44</sup> In this experiment, 10 mol % of **1**, 1 equiv. of styrene, and 1 equiv. of *para*-substituted styrene were treated with 0.8 equiv. of phenylphosphine under photocatalytic conditions. Relative conversion was determined after 30 min by <sup>1</sup>H NMR spectroscopy, and each reaction was performed in duplicate or triplicate (See SI for details). A negative  $\sigma$  was found for electron-donating substituents, and a positive  $\sigma$  was found for electron-withdrawing substituents, which yielded a divergent (concave) Hammett plot (Figure 1). Identical behavior was observed when Ph<sub>2</sub>PH was used in the reaction (Figure S7). A concave Hammett plot typically indicates a change in mechanism upon introduction of different substituents.<sup>45</sup> Interestingly, this divergence is consistent with the high activity of **1** towards both electron rich and poor unsaturated substrates.<sup>37</sup> The high activity of **1** towards electron-poor substrates is likely a nucleophilic attack of a copper phosphido on an unsaturated substrate, the operant mechanism of many late-metal hydrophosphination catalysts.<sup>8</sup> However, the high activity of **1** towards unactivated substrates is inconsistent with a nucleophilic mechanism. For example, 1-hexene is unlikely to be subject to nucleophilic attack.<sup>37</sup> Precedent for an insertion pathway with copper comes from Cui and Whittlesey who have previously proposed insertion of terminal alkynes<sup>46</sup> and isocyanates,<sup>16</sup> respectively, into the Cu–P bond of NHC-copper phosphido compounds. Therefore, an initial hypothesis for this divergence, a combination of nucleophilic and insertion steps, was formed. However, these data are unable to exclude a radical pathway, and testing this possibility was necessary.

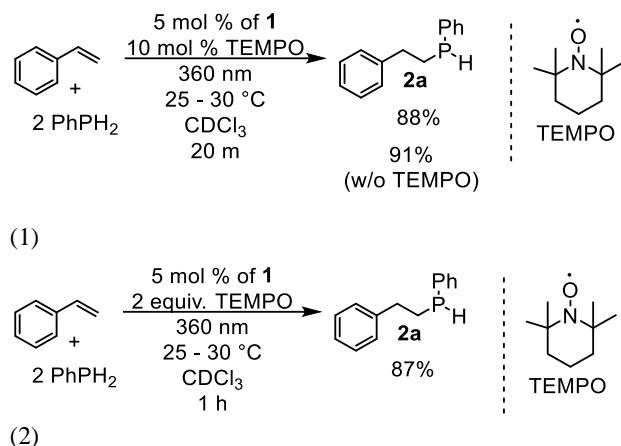
**Figure 1.** Hammett study of *para*-substituted styrene derivatives and PhPH<sub>2</sub> with **1**.



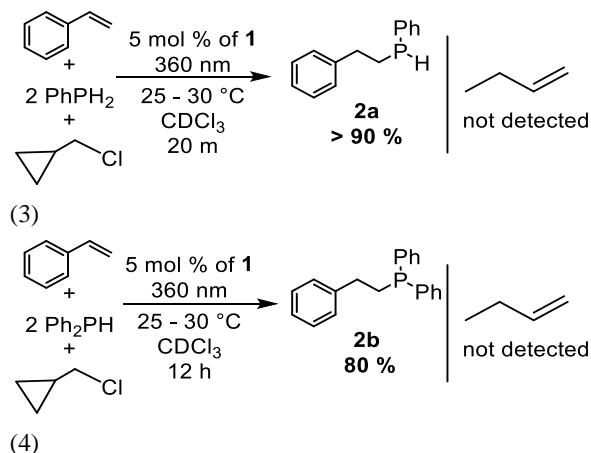
### Evidence supporting a homogenous, two-electron process

The assertion that two potential mechanisms are operating made identifying or eliminating radical and/or heterogenous catalysis urgent. Additionally, a clearer answer on this issue would inform if a prefabricated copper(I) pre-catalyst would be a good proxy for **1** in further study. To detect radical reactivity, several experiments were performed. As an initial test, a reaction with 2 equiv. of phenylphosphine with styrene and 5 mol % of **1** was conducted in the presence of 10 mol % of 2,2,6,6-tetramethylpiperidine-N-oxyl (TEMPO)<sup>47</sup> under photocatalytic conditions (Eq 1). Complete conversion of styrene with 88% selectivity for the anti-Markovnikov single addition hydrophosphination product **2a** was observed. This compares favorably to a reaction conducted without TEMPO where full conversion of styrene with 91% selectivity for **2a** was observed.<sup>37</sup> The lack of inhibition from TEMPO is inconsistent with a radical based process. However, a complicating factor is that TEMPO can react directly with phosphines,<sup>48, 49</sup> and the possibility existed that the lack of inhibition was the result of complete consumption of TEMPO before it could react with the catalyst. To test for this possibility, a replicated reaction with 2 equiv. of TEMPO was performed to increase the likelihood of direct reaction of TEMPO with the catalyst (Eq 2). As expected, an initial <sup>31</sup>P{<sup>1</sup>H} NMR spectrum of only phenylphosphine and TEMPO in CDCl<sub>3</sub> revealed consumption of 17% of phenylphosphine and the formation of several TEMPO-based byproducts. After addition of styrene and 5 mol % of **1**, 26% of the phosphine had reacted to form byproducts. When this reaction was irradiated, the system remained active with 87% conversion within 1 h. While this is

slower than the reaction without TEMPO, the decreased concentration of phosphine due to reaction with TEMPO is a strong factor. Catalyst deactivation would result in lower conversions, based on control reactions.



The possibility remained that TEMPO may be regulating the radical flux of a phosphorus-based radical ( $[P] + \text{TEMPO} \rightleftharpoons \text{TEMPO}[P]$ ) in solution as suggested by Knights et al.<sup>50</sup> To detect a phosphorus-based radical, a trap that does not interact with phosphine was selected. Two equiv. of phenylphosphine, styrene, and 5 mol % of **1** were allowed to react in the presence of 1 equiv. of (chloromethyl)cyclopropane under photocatalytic conditions (Eq 3). Observed reactivity was identical to the reaction conducted without (chloromethyl)cyclopropane. Full conversion of styrene with greater than 90% selectivity for **2a** was measured within 20 min upon irradiation. Importantly, the (chloromethyl)cyclopropane remained intact. No 1-butene was detected (as measured by NMR spectroscopy), as can occur in the presence of a radical and was observed in radical hydrophosphination reactions reported by Webster.<sup>19</sup> Full consumption of styrene and 80% conversion to **2b** with no detectable 1-butene occurred in a replication of this experiment with diphenylphosphine after 12 h of irradiation (Eq 4).



Further evidence against the presence of radicals in this catalysis came from an in-situ EPR experiment that mirrors one performed by Corma with  $\text{Cu}(\text{OTf})_2$ .<sup>39</sup> Treatment of a toluene solution of  $\text{PhPH}_2$  and *p*-tert-butyl styrene with 5 mol % of **1** resulted in the loss of signal for **1** as measured by EPR spectroscopy (See SI for additional details). Subsequent in situ

irradiation at 360 nm for 30 min and monitoring by EPR spectroscopy did not result in any detectable signal. NMR spectra of this reaction mixture demonstrated complete conversion to product. These results suggest an in-situ reduction of  $\text{Cu}(\text{II})$  gives a  $\text{Cu}(\text{I})$  active catalyst that proceeds in closed shell reaction steps.

In some examples, **1** is a precursor to copper oxide nanoparticles in the presence of various organic substrates under thermal conditions.<sup>51, 52</sup> Several observations argue against this pathway. Previous reports of nanoparticle formation result in the formation of acetic acid and acetone byproducts that are not detected in this system.<sup>51</sup> As a test of homogeneity of the active catalyst, 450 mg of elemental mercury (Hg) was added to sequester any precipitated copper in the reaction of  $\text{Ph}_2\text{PH}$  and styrene and catalyzed by 5 mol % of **1** in chloroform-*d*<sub>1</sub>.<sup>47</sup> Observed reactivity was identical to reactions conducted without added Hg, suggesting that copper(0) is not precipitating, which is also consistent with visual observation of a homogenous system. While these data are not definitive,<sup>53</sup> they are consistent with molecular catalysis.

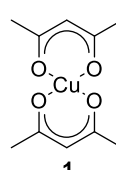
### Testing precursors and verifying copper(I)

With good indications of homogeneity and closed-shell reactivity, several copper pre-catalysts were then tested to probe for differences based on supporting ligand, counter ion, and oxidation state. To test the role of the  $\beta$ -diketonate ligand in the reaction, the reactivity of copper(II) bis(2,2,6,6-tetramethyl-3,5-heptanedionate) (**3**) and copper(II) bis(2,2,6,6-tetrafluoro-3,5-heptanedionate) (**4**) were explored (Table 1). When styrene was treated with 2 equiv. of phenylphosphine and 5 mol % of **1** or **3** under photocatalytic conditions, almost identical reactivity was observed with both compounds, affording quantitative conversion within 20 min (Table 1, entries 1 and 2). Diminished reactivity was observed when this reaction was conducted with 5 mol % of **4**, where only 30% conversion of styrene (Table 1, entry 3) was measured in the same reaction time. The same trend was observed in reactions with 1-hexene in which greater than 70% conversion was observed with compounds **1** and **3** (Table 1, entries 4 and 5) compared to 44% conversion with compound **4** (Table 1, entry 6). A control reaction omitting copper gave 4% conversion under irradiation (Table 1, entry 7). Additionally, <sup>1</sup>H NMR signals attributed to acetylacetone or 2,2,6,6-tetramethyl-3,5-heptanedione were detected in reaction mixtures with **1** and **3** respectively, but the corresponding  $\beta$ -diketone, 1,1,1,5,5,5-hexafluoroacetylacetone, was not observed in NMR spectra of reaction mixtures with **4**. The decreased reactivity of **4** is thus attributed to slower protonation of the less basic  $\beta$ -diketonate ligand, resulting in slower catalyst activation. This comparative analysis demonstrates how composition of the copper(II) compound is important for catalysis and is one indication of how the counterion can distinctly influence catalytic performance for a copper(II) precatalyst.

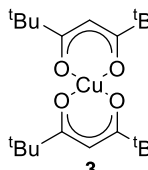
**Table 1. Comparison of copper(II) bis( $\beta$ -diketonato) precursors**

$$\text{R} \sim + 2 \text{ PhPH}_2 \xrightarrow[25-30^\circ\text{C}]{5 \text{ mol \% of [Cu]}, 360 \text{ nm}, \text{CDCl}_3} \text{R} \sim \text{P}(\text{Ph})_2$$

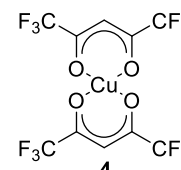
| Entry | [Cu]     | Time | alkene   | Conv. % |
|-------|----------|------|----------|---------|
| 1     | <b>1</b> | 20 m | styrene  | 100     |
| 2     | <b>3</b> | 20 m | styrene  | 100     |
| 3     | <b>4</b> | 20 m | styrene  | 30      |
| 4     | <b>1</b> | 20 h | 1-hexene | 80      |
| 5     | <b>3</b> | 24 h | 1-hexene | 72      |
| 6     | <b>4</b> | 24 h | 1-hexene | 44      |
| 7     | None     | 24 h | 1-hexene | 4       |



**1**



**3**



**4**

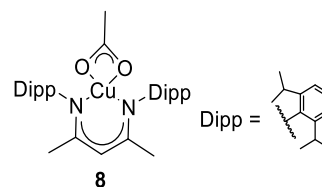
Additional copper precatalysts were screened under photocatalytic conditions that included Lipshutz's previously reported copper(II) acetate monohydrate ( $\text{Cu}(\text{OAc})_2 \cdot \text{H}_2\text{O}$ , **5**),<sup>40</sup> copper(I) oxide ( $\text{Cu}_2\text{O}$ , **6**), tetrakis(acetonitrile)copper(I) hexafluorophosphate ( $[\text{Cu}(\text{CH}_3\text{CN})_4]\text{PF}_6$ , **7**), and a  $\beta$ -diketiminato copper(II) compound (**8**). All copper catalysts tested were successful at catalyzing the hydrophosphination of styrene and phenylphosphine, at varying relative rates, under the same photocatalytic conditions (Table 2, entries 1-4). Copper(I) compounds **5**, **6**, and **7**, were also active with 1-hexene to various degrees (Table 2, entries 5-7). The difference in apparent relative rates is likely to be a result of differing rates of activation, which reiterate the likely role of ancillary ligand basicity in activation to initially reduce copper(II) as much to activate copper(I). For example, **6** is insoluble but over time the appearance of phosphine oxides detectable by  $^{31}\text{P}\{^1\text{H}\}$  NMR spectroscopy in reaction mixtures with **6** suggest oxygen transfer from copper and the formation of a soluble copper species. Phosphine oxides are not detectable in reactions with **1**. In a similar vein, addition of Proton sponge (1,8-dimethylamino naphthalene) to a reaction catalyzed by **7** improved reactivity. This is likely due to deprotonation of a coordinated phosphine to form a copper phosphido due to the weak basicity of  $\text{PF}_6^-$  (Table 2, entry 8). A similar observation was made by Lin.<sup>25-26</sup> Of note, a prefabricated copper(II) compound, **8**, was entirely inert in the hydrophosphination of 1-hexene (Table 2, entry 9). Taken together, these data not only provide additional support for a copper(I) phosphido active species, but more importantly, they demonstrate the generalizability of photocatalysis with various copper precursors that are capable of being activated (often via protonation) to soluble copper(I) active catalysts.

**Table 2. Comparison of other copper precursors**

$$\text{R} \sim + 2 \text{ PhPH}_2 \xrightarrow[25-30^\circ\text{C}]{5 \text{ mol \% of [Cu]}, 360 \text{ nm}, \text{CDCl}_3} \text{R} \sim \text{P}(\text{Ph})_2$$

| Entry | [Cu]  | Time | Alkene   | Conv. % |
|-------|---|------|----------|---------|
| 1     | $\text{Cu}(\text{OAc})_2$ ( <b>5</b> )              | 20 m | styrene  | 86      |
| 2     | $\text{Cu}_2\text{O}$ ( <b>6</b> )                  | 20 m | styrene  | 15      |
| 3     | $\text{Cu}(\text{MeCN})_4 \text{PF}_6$ ( <b>7</b> ) | 20 m | styrene  | 45      |
| 4     | <b>8</b>  | 20 m | styrene  | 41      |
| 5     | <b>5</b>  | 20 h | 1-hexene | 68      |
| 6     | <b>6</b>  | 24 h | 1-hexene | 73      |
| 7     | <b>7</b>  | 16 h | 1-hexene | 26      |
| 8     | <b>7</b> <sup>a</sup>                               | 16 h | 1-hexene | 67      |
| 9     | <b>8</b>  | 24 h | 1-hexene | 1       |

[a] 40 mol % of 1,8-bis(dimethylamino)naphthalene.

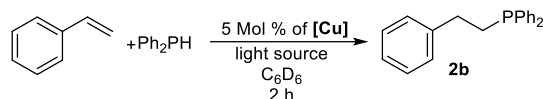


#### Model reactions with $\text{IPrCuPPh}_2$

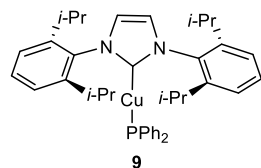
With data to support a soluble, closed-shell process and generalizable copper photocatalysis, a suitable molecular model system was pursued to provide greater understanding of this catalysis. Such a discrete molecular compound catalyst is attractive because polymetallic copper phosphido compounds have also been demonstrated to be effective pre-catalysts for this hydrophosphination<sup>41,43</sup> but are more challenging for study. To identify a discrete copper(I) phosphido compound for further study, several catalytic reactions were attempted with the known derivative  $\text{IPrCuPPh}_2$  (**9**) (Table 3). Compound **9** is a monomeric phosphido compound, originally prepared by Nolan,<sup>54</sup> that has been structurally characterized and demonstrated to catalyze the hydrophosphination of isocyanates by Whittlesey under ambient light.<sup>16</sup> For these reasons, **9** was an attractive compound to test for photocatalytic reactivity. Styrene was treated with 1 equiv. of diphenylphosphine and 5 mol % of **9** under photocatalytic conditions as shown in Table 3. When irradiated with a 360 nm-centered commercial lightbulb, 45% conversion was observed after 2 h as determined by  $^1\text{H}$  and  $^{31}\text{P}\{^1\text{H}\}$  NMR spectroscopy (Table 3, entry 1). Comparable conversions were measured with a commercial "blacklight" near-UV LED bulb or a strip of blue light LED bulbs (Table 3, entries 2 and 3), demonstrating the generality of simple light sources. When irradiated with a 23 W CFL bulb, there was greater than 90% conversion to the tertiary phosphine product measured for **9** versus 80% for **1** over the same time period (Table 3, entries 4 and 5), a difference that is attributed

to the activation step necessary for **1**. The same reaction conducted under ambient light or in the dark resulted in only 13% and 0% (Table 3, entries 6 and 7) conversion, respectively. A control reaction omitting copper gave 8% conversion under irradiation (Table 3, entry 8). These reactions reiterate the importance of light in catalysis with both **1** and **9**. More germane, the similarity in activity between **1** and **9** indicates that a monomeric copper phosphido compound is an active intermediate and that **9** can be a useful tool in understanding photocatalytic hydrophosphination using copper.

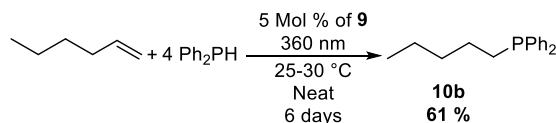
**Table 3. Comparative hydrophosphination of styrene to establish the utility of monomeric compound **9****



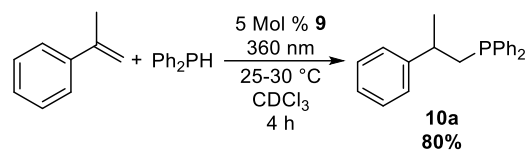
| Entry | [Cu]     | Light Source   | Conversion % |
|-------|----------|----------------|--------------|
| 1     | <b>9</b> | 360 nm         | 45           |
| 2     | <b>9</b> | blacklight LED | 44           |
| 3     | <b>9</b> | blue LED       | 77           |
| 4     | <b>9</b> | 23 W CFL       | 91           |
| 5     | <b>1</b> | 23 W CFL       | 80           |
| 6     | <b>9</b> | ambient        | 13           |
| 7     | <b>9</b> | dark           | 0            |
| 8     | none     | 23 W CFL       | 8            |



To further confirm **9** is a valid catalyst for study, two more difficult substrates were attempted. Treatment of a chloroform-*d*<sub>1</sub> solution of  $\alpha$ -methylstyrene, diphenylphosphine, and 5 mol % of **9** under 360 nm irradiation resulted in 80% conversion to **10a** as determined by <sup>1</sup>H NMR spectroscopy (Eq 6). Interestingly, compound **9** was more active than **1** under the same conditions. However, not all substrates were faster with **9**. A neat solution of 4 equiv. of diphenylphosphine and 1-hexene in the presence of 5 mol % of **9** resulted in 18% conversion to **10b** after 18 h and 61% conversion after 6 days of irradiation (Eq 5). This is a slower apparent rate than was previously observed with **1** which had 64% conversion with 3 equiv. of phosphine after 24 h. While the lack of an activation step and the steric and electronic contributions of the ancillary NHC ligand undoubtedly affects the rate of reactivity, it is apparent that **9** is a valid hydrophosphination photocatalyst precursor and a valid proxy for **1** in continued study.



(5)

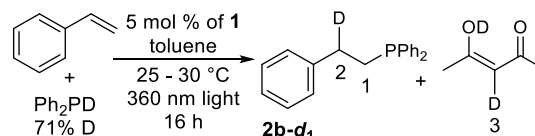


(6)

## Deuterium labeling experiments

Deuterium labeling experiments were performed to better understand selectivity in the key bond formation steps of the catalysis. Styrene was treated with one equiv. of phenylphosphine-*d*<sub>1</sub> (71% deuterium) and 5 mol % of **1** under irradiation and monitored by <sup>1</sup>H, <sup>2</sup>H, and <sup>31</sup>P{<sup>1</sup>H} NMR spectroscopy (Figure 2). After 16 h, 86% conversion to product **2b-d**<sub>1</sub> was observed with 58% deuterium enrichment at the carbon adjacent to the phenyl substituent (C2, Figure 2), accounting for 81% of the added deuterium. The balance, or approximately 18% of the deuterium, was observed at oxygen and the methylene carbon (C3, Figure 2) of acetylacetone. This observation explains the lack of complete deuterium incorporation on the hydrophosphination product. The remaining trace deuterium was present in oxidized starting material Ph<sub>2</sub>P(O)H. Multiple deuterium exchanges at acetylacetone indicate that there is more complex chemistry associated with this ligand. However, critical transfer of hydrogen in hydrophosphination appears to be affiliated with an ordered process exclusively at the 2-position from these data.

**Figure 2. Deuterium labeling experiment**

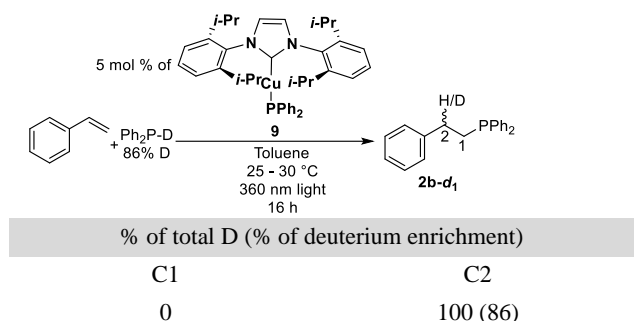


% of total D (% of deuterium enrichment)

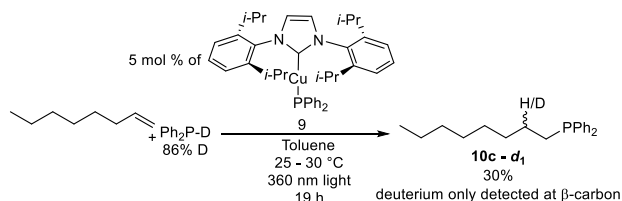
| C1 | C2      | C3       | O        |
|----|---------|----------|----------|
| 0  | 81 (58) | 9.2 (92) | 9.2 (92) |

In light of this complexity, a second deuterium labeling experiment was performed with **9** as catalyst. Styrene was treated with 1 equiv. of Ph<sub>2</sub>PD (86% deuterium) and 5 mol % of **9** under 360 nm irradiation in toluene and replicated in toluene-*d*<sub>8</sub> (Figure 3). After 24 h, 69% conversion had occurred with the only detectable deuterium at C2 of the tertiary phosphine product, **2b-d**<sub>1</sub>, as measured by <sup>1</sup>H, <sup>2</sup>H, and <sup>31</sup>P{<sup>1</sup>H} NMR spectroscopy. Deuterium was not detected at any other position of the product.

**Figure 3.** Deuterium labeling experiment with **9**



A similar experiment in which a neat solution of 1-octene and 3 equiv. of  $\text{Ph}_2\text{PD}$  were allowed to react with 5 mol % of **9** resulted in 30% conversion as determined by  $^{31}\text{P}\{^1\text{H}\}$  NMR spectroscopy after 19 h (Eq 7). In this experiment, deuterium was only detectable at the  $\beta$ -carbon relative to phosphorus in the  $^2\text{H}$  NMR spectrum. However, an accurate determination of the amount of deuterium versus hydrogen at this position (i.e., percent of product deuteration) was not discernable from a  $^1\text{H}$  NMR spectrum due to overlap with protons on the  $\gamma$ -carbon.

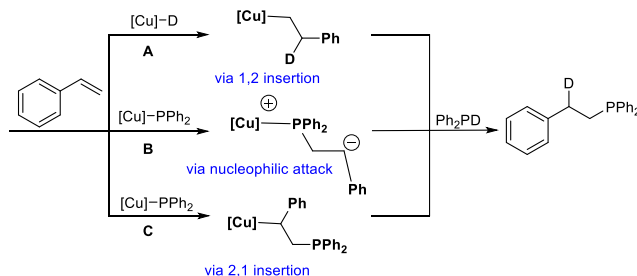


(7)

The observed isotopomers are consistent with three potential reaction pathways (Scheme 1). Path A, migratory insertion of alkene into a copper hydride, can be eliminated immediately for three reasons. First, treatment of copper hydrides with diphenylphosphine results in the rapid formation of a copper phosphido.<sup>38</sup> Second, the activation process for **1** requires H-transfer to the acetylacetonate (acac) ligand to form a copper phosphido, rather than a hydride, based on analysis of byproducts, which is consistent with deuteration at C3 of acetylacetone (Figure 2). Third, results from Buchwald in copper-catalyzed hydroamination and Hartwig in copper-hydride hydroboration indicate 2,1-insertion of styrene into a copper hydride is favored over the 1,2 insertions.<sup>55, 56</sup> In path B, a copper phosphido could perform nucleophilic attack on alkene substrate to form a zwitterionic intermediate and then undergo protonation (Scheme 1, path B). While this path is possible for Michael acceptors and even styrene, the experiments with 1-hexene and 1-octene demonstrate that this is not feasible for all substrates. The final possibility is a 2,1-insertion of substrate followed by protonation (Scheme 1, path C). This is the most favorable possibility for two reasons. First, the 2,1-insertion accounts for the anti-Markovnikov selectivity observed in the catalysis regardless of substrate. Second, this pathway allows for the selectivity in deuteration observed for unactivated alkenes like 1-hexene. Thus, deuterium labeling supports 2,1-insertion of unactivated alkenes, which may also be possible for Michael acceptors. However, these data do not account for a mechanistic distinction in P–C bond formation. Therefore,

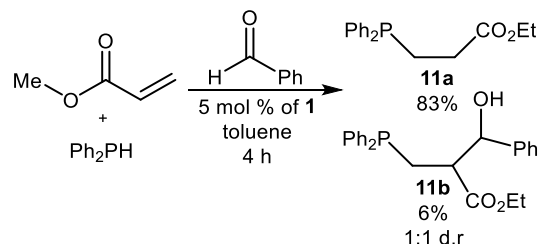
additional experimentation is needed to account for the divergence in mechanism from Hammett data.

**Scheme 1.** Three potential mechanisms that provide product selectivity observed in deuterium labeling experiments



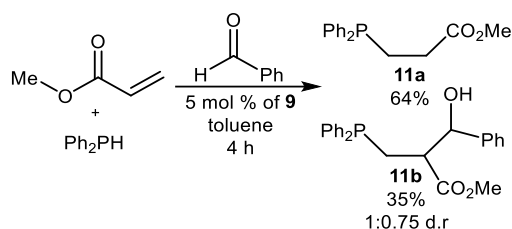
#### Evidence for a zwitterionic intermediate

Electron-deficient alkenes are likely subject to nucleophilic attack based on literature precedent.<sup>8, 15, 57-59</sup> Indeed, small amounts of telomerization products observed in the reaction of diphenylphosphine and acrylonitrile in the presence of **1** that indicate that a zwitterionic intermediate similar to that reported by Glueck for platinum-catalyzed hydrophosphination.<sup>8, 57</sup> To test for this mechanism, a trapping experiment mirroring one executed by Glueck was performed. A reaction of diphenylphosphine, methyl acrylate, and 5 mol % of **1** was treated with excess (5 equiv.) of benzaldehyde in an effort to trap a zwitterionic intermediate (Eq 8). After 4 h, the hydrophosphination product, **11a**, was the major product in greater than 13:1 ratio, with 6% conversion to the three-component coupling product, **11b**, as determined by  $^{31}\text{P}\{^1\text{H}\}$  NMR spectroscopy (Eq 8). When this experiment was replicated with compound **9**, the hydrophosphination product **11a** was the major product but in only a 2:1 ratio compared to **11b** (Eq 9). The formation of **11b** suggests that a zwitterionic intermediate is in solution in catalysis with **1** and **9**. The decreased formation of **11a** observed with **1** as catalyst may be a result of benzaldehyde inhibiting the formation of a copper phosphido in contrast to the prefabricated copper phosphido of **9**. With both **1** and **9**, there is significantly less trapping product (i.e., **11b**) formed than was observed by Glueck in the platinum system where the major product was trapping by a 3:1 ratio.<sup>57</sup> The decreased formation of trapped product with copper suggests that the zwitterionic intermediate is likely longer lived with platinum and therefore subject to more trapping. Most important, the trapping reactions are consistent with a nucleophilic attack at electron deficient unsaturated substrates.



(8)





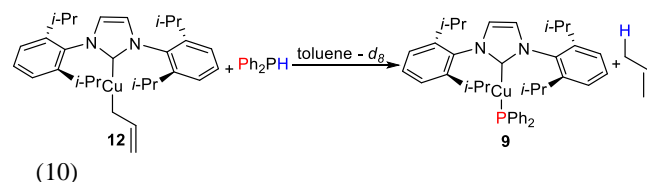
(9)

### Attempted observation of insertion products

To test for alkene insertion into the Cu–P bond, **9** was treated with 1 equiv. of styrene in benzene-*d*<sub>6</sub> then irradiated at 360 nm and monitored by <sup>1</sup>H, <sup>31</sup>P{<sup>1</sup>H}, and <sup>31</sup>P HMBC NMR spectroscopy. Unfortunately, these efforts failed to provide clear data for a stoichiometric insertion into the Cu–P bond, rather mixtures of products that could not be conclusively assigned were instead observed. Two points are of note in this effort. First, many alkyl peaks were measured that are correlated with phosphorus shifts in a <sup>31</sup>P HMBC NMR spectrum. Second, no reaction occurs in the absence of light, even with a large excess of styrene, when monitored over the same time frame. Similar results were obtained in identical experiments with *para*-methoxy styrene, norbornene, or with irradiated neat mixtures of **9** with excess ethyl vinyl ether or 1-hexene (See SI for details), all consistence with the need for light in the pathway of electron-rich substrates.

### C–H bond formation

In both insertion and zwitterionic mechanistic pathways, the phosphine product is likely released and the copper phosphido is restored by formal protonation of an intermediate Cu–C bond by primary or secondary phosphine. To confirm the viability of this step, alkyl copper compound IPrCu(CH<sub>2</sub>CH=CH<sub>2</sub>) (**12**)<sup>60</sup> was treated with 1 equiv. of diphenylphosphine in a benzene-*d*<sub>6</sub> solution. A signal at δ = –26 corresponding to compound **9** was observed in the <sup>31</sup>P{<sup>1</sup>H} NMR spectrum, and formation of propylene was confirmed in the <sup>1</sup>H NMR spectrum (Eq 10). Repetition of the experiment with phenylphosphine gave analogous results, confirming that primary and secondary phosphine can protonate an alkyl copper compound to form/restore a phosphido compound.

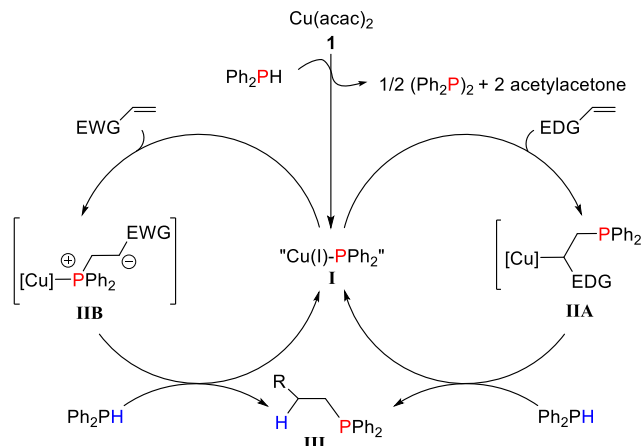


(10)

### Proposed catalytic cycle

Taken all together, the above data point to two catalytic cycles. Initially, **1** is reduced by a primary or secondary phosphine to generate an active copper(I)-phosphido compound (**I**, depicted with Ph<sub>2</sub>PH for simplicity), 2 equiv. of acetylacetonate, and 0.5 equiv. of 1,2-tetraphenyldiphosphine (Scheme 3). As identified, discrete copper(I) compounds circumvent this activation step. In the presence of electron rich alkenes, a 2,1-insertion into the copper–phosphorus bond occurs to form an alkyl copper species releases the hydrophosphination

product (**III**) and reforms the copper phosphido **I**. In the presence of electron deficient alkenes, **I** may engage in nucleophilic attack to generate a zwitterionic intermediate (**IIB**). Protonation of **IIB** forms hydrophosphination product (**III**) and regenerates the copper-phosphido catalyst. This mechanistic proposal reconciles experimental observations of the catalysis, stoichiometric reactions, Hammett data, and model transformations with copper(I) compounds. Some questions remain, chief among them is, what is the role of light?



**Scheme 3.** Proposed mechanism of copper-catalyzed hydrophosphination

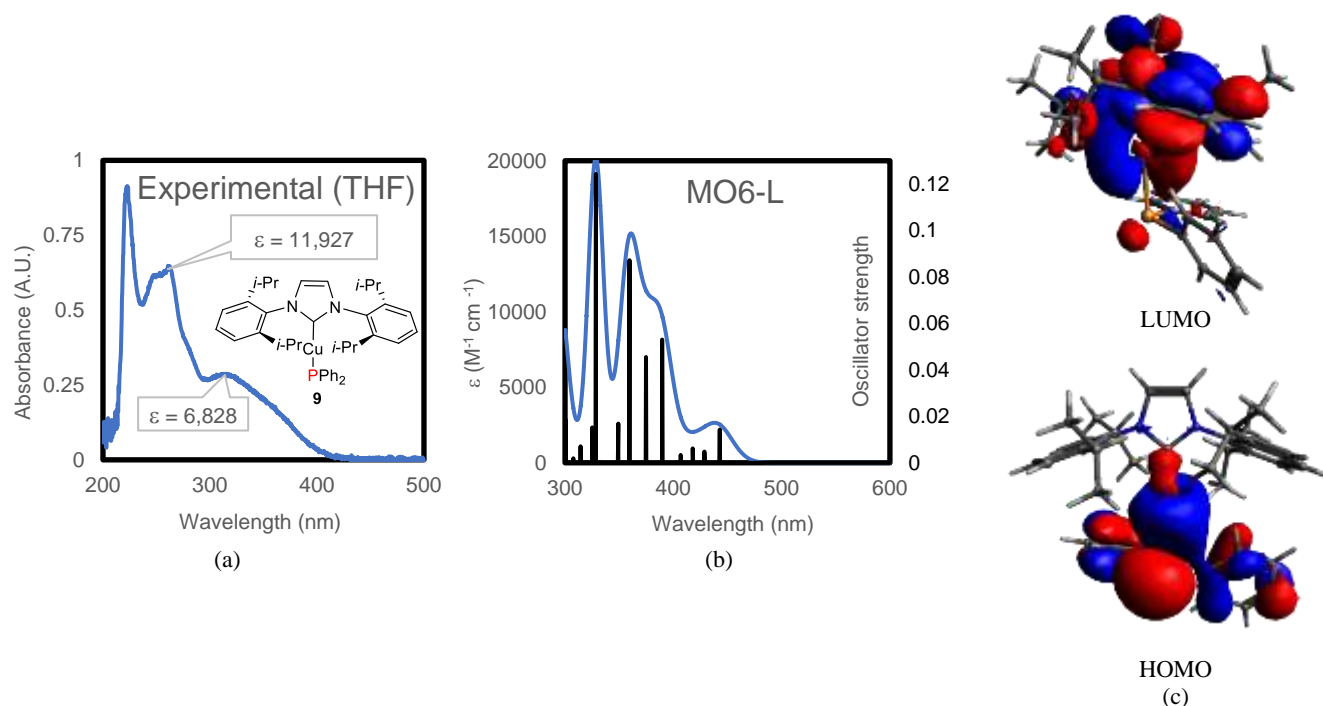
### Computational analysis/Role of light

While these data are informative, they do not explain the role of light. The phenomenon of photocatalytic hydrophosphination has been described. In particular, photocatalytic hydrophosphination with zirconium appears to depend on a P n → Zr d LMCT that results in the lengthening of the Zr–P bond to promote facile substrate insertion.<sup>61, 62</sup> This seemingly benign transition results in bond elongation due to significant Zr–P antibonding character of the acceptor orbital. To probe for a potentially related phenomenon with copper, compound **9** was explored by spectroscopic and computational analyses.

UV-visible spectra of **9** were obtained as THF solutions (Figure 4a). Absorption bands were observed at 225 nm, 265 nm, and 320 nm (See SI for additional details). The band of interest at 320 nm is broad and trails past 400 nm, which is consistent with the yellow color of these compound and reactions. These primarily ultraviolet transitions that have a non-trivial cross section in the visible also explain activity observed with copper across a variety of wavelengths. The nature of the lowest energy transition was of keen interest from prior work that suggests copper compounds obey Kasha's Rule.<sup>63</sup>

Investigation of **9** via DFT computations were performed. Benchmarked computations for copper phosphido compounds of this general type were not found in the literature. Thus, the ground state geometry of **9** was optimized with the functionals PBE, PBEO, BLYP, B3LYP, and MO6-L using the def2-TZVP basis set. These optimized structures are in good agreement with the molecular structure of **9** reported by Whittlesey from an X-ray diffraction study (See SI for details) and were explored via TD-DFT modeling.<sup>16</sup>

**Figure 2.** a) Experimental UV-visible spectra of **9** in THF b) Calculated UV-visible spectra of **9** in THF with MO6-L/ def2-TZVP c) HOMO and LUMO of **9** calculated with MO6-L/ def2-TZVP



The absorption intensities of **9** were performed using the PBE, PBE0, BLYP, B3LYP, MO6 and MO6-L functionals with Gaussian and analyzed with GaussSum at 1500  $cm^{-1}$  fwhm. The computed UV-vis spectra from PBE, BLYP, B3LYP, and MO6-L were all in good agreement with the experimental UV-vis spectra as measured by the intensities and distance between the two lowest energy transitions. BLYP most accurately predicted the relative intensities of the two peaks predicting an approximately 2:1 ratio and slightly overestimated the 60  $cm^{-1}$  distance between two peaks. Whereas the spectrum calculated with MO6-L accurately predicted a 60  $cm^{-1}$  difference between the two peaks and slightly overestimated the difference in band intensities. All four of these spectra revealed a low-energy band composed predominantly of a single electronic transition followed by a higher energy band composed of several electronic transitions. For simplicity, MO6-L is depicted in Figure 4b, but the complete analysis can be found in the Supporting Information.

With all four functionals, the low energy band computed by TDDFT was found to be a one electron excitation with 93–98% HOMO→LUMO character. Visual inspection of the orbitals computed from all four functionals revealed a phosphorus-dominated HOMO with a LUMO that appeared to have more copper character but was distinctly Cu–P antibonding in appearance (Figure 4c). Mulliken orbital populations confirmed this coarse analysis. The HOMO is predominantly composed of the phosphorus 4  $P_z$  and 5  $P_z$  atomic orbitals and the largest contributors to the LUMO are from the NHC carbon and the Cu 4 $P_z$  atomic orbitals. These ground state computations are suggestive of

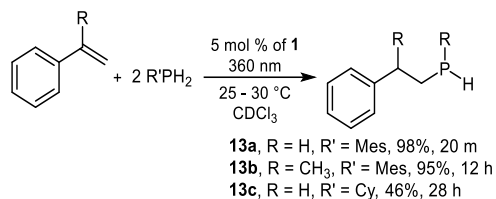
a single electron excitation that populates an orbital that would weaken the copper–phosphido bond. Unfortunately, optimization of the excited state geometry did not converge on a one electron excitation. Nevertheless, computational data gives a strong preliminary indication that photoexcitation for copper may facilitate insertion via weakening of the Cu–P bond, as has now been seen for several zirconium compounds.<sup>61, 62</sup> Most germane to catalysis, it suggests that this photoactivity is substrate independent and new, challenging substrates can be realized via photocatalytic hydrophosphination using copper.

#### Hydrophosphination of difficult substrates

With this improved mechanistic understanding, expansion of this catalysis to address challenges in hydrophosphination are underway. One articulated challenge is the absence of variety in the phosphorus substituents where  $Ph_2PH$ , and more recently  $PhPH_2$ , are the most commonly reported substrates.<sup>12, 17, 31, 64, 65</sup> For copper, preliminary data indicates more diverse phosphine substrates are viable. Treatment of styrene with 2 equiv. of mesitylphosphine in the presence of 5 mol % of **1** gave quantitative conversion to product **13a** within 20 min. Treatment of 2 equiv. of mesitylphosphine with  $\alpha$ -methyl styrene resulted in greater than 95% conversion to the novel product **13b** after 12 h of 360 nm irradiation. Two equivalents were not required for selectivity as the same reaction with 1 equiv. went to 59% conversion over the same time frame and 79% conversion (61% isolated yield) after 36 h with only trace detection of the double P–H bond activation product. Reaction of 2 equiv. of cyclohexylphosphine with styrene and 5 mol % of **1** proceeded to 46% conversion to product **13c** after 28 h of

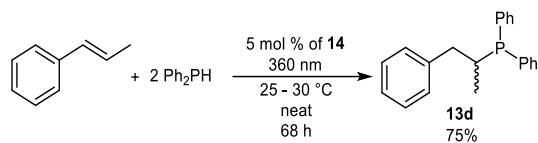


360 nm irradiation (Eq 11). The apparently lower activity of CyPH<sub>2</sub> in comparison to aryl phosphines is interesting and in need of deeper investigation. Clearly, more substrate scope exploration is needed, but these results demonstrate the capacity for copper to engage in a broader scope, especially leveraging the greater reactivity afforded by photocatalysis.



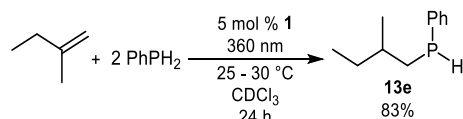
(11)

A second, larger challenge in hydrophosphination is the poor tolerance for sterically encumbered alkenes. For example, there are only two prior reports of the hydrophosphination of  $\beta$ -methyl styrene with diphenylphosphine and each required temperatures of 100 °C with 41% the highest yield achieved by a cerium MOF after 5 days of heating.<sup>18, 39</sup> Under 360 nm irradiation at ambient temperature, hydrophosphination of a neat mixture of *cis/trans*  $\beta$ -methyl styrene with diphenylphosphine in the presence of 5 mol % of CuOAc (**14**) proceeds to 73% conversion to product **13d** in less than 3 d (Eq 12). Compound **1** achieves 25% conversion under the same conditions after 3 d, demonstrating how even simple prefabricated copper(I) can be valuable in saving the catalytic activation step in these longer reactions.

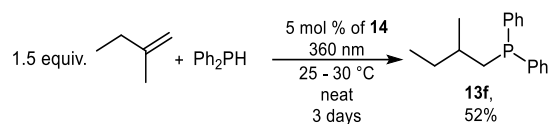


(12)

Hydrophosphination of  $\alpha$ -substituted unactivated alkenes, to our knowledge, has not been reported with primary phosphines, and the known example is, again, Lin's cerium MOF using secondary phosphines.<sup>18</sup> Treatment of 2-methyl-1-butene and 2 equiv. of phenylphosphine with 5 mol % of **1** afforded 83% conversion to **13e** after 24 h of irradiation (Eq 13). A reaction with 1 equiv. of diphenylphosphine and 1.5 equiv. of 2-methyl-1-butene resulted in 38% conversion (with respect to phosphine) to product **13f** after 3 d of irradiation. Again, faster reactivity can be achieved with prefabricated Cu(I) compound **14** as the same reaction but with 5 mol % of **14** resulted in 52% conversion after 3 d of irradiation (Eq 14). Excess 2-methyl-1-butene was utilized due to this substrate's volatility to ensure adequate substrate in solution through the course of the reaction. These are improvements in reactivity with challenging substrates, but more work is needed.

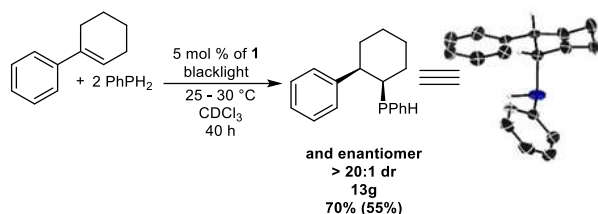


(13)



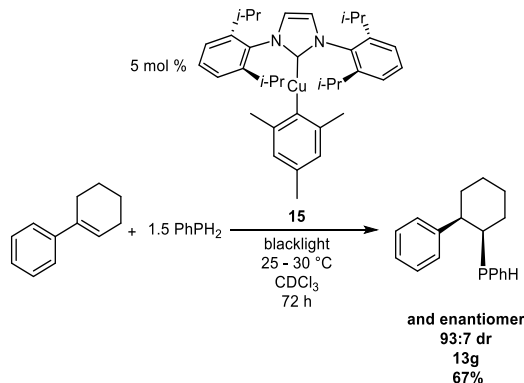
(14)

Recognizing the potential enhancement of reactivity via photocatalysis using copper, a tri-substituted styrene was screened with copper. Treatment of 1-phenyl-1-cyclohexene with 2 equiv. of phenylphosphine under 360 nm irradiation in the presence of 5 mol % of **1** gave 36% conversion to **13e** after 48 h. Under greater irradiation, from two side-by-side commercially available blacklights, a similar reaction resulted in 70% NMR conversion and 55% isolated yield after 40 h (Eq 15). This demonstrates that photon density may be the key factor to coaxing greater activity and thereby substrate scope from copper hydrophosphination catalysts. Greater than 20:1 selectivity for the *cis*-diastereomer (i.e., that resulting from a net trans addition of the P-H bond) was detectable by <sup>1</sup>H and <sup>31</sup>P{<sup>1</sup>H} NMR spectroscopy. This assignment was confirmed by single crystal X-ray analysis of crystals of **13e** grown from a concentrated pentane solution at -30 °C. To our knowledge, no tri-substituted styrene has been functionalized in any previous hydrophosphination reports.

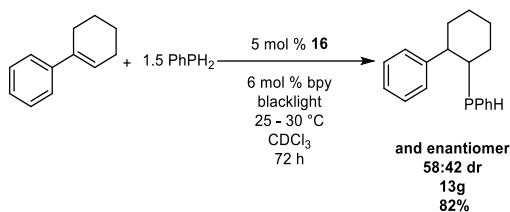


(15)

In an initial test of the effect of a supporting ligand on diastereoselectivity, 1-phenyl-1-cyclohexene was treated with 1.5 equiv. of phenylphosphine and 5 mol % of IPrCuMes (**15**) under irradiation, which resulted in 67% conversion with 93:7 d.r for the *cis* product (Eq 16). A second experiment was conducted under identical conditions but with 2 equiv. of phenylphosphine and in the presence of 5 mol % of mesityl copper(I) (**16**) and 2,2'-bipyridine (bpy) that gave 82% conversion after 72 h with a 58:42s d.r (Eq 17). These results demonstrate that the careful choice of ligand allows for diastereoselectivity with this substrate. Optimization to select for the *trans*-isomer and further exploration of both stereo- and enantioselectivity is ongoing.



(16)



(17)

## CONCLUDING REMARKS

A series of studies were conducted that address the key mechanistic steps in copper-catalyzed hydrophosphination. These data support a copper(I) active catalyst that proceeds via either an insertion-based or nucleophilic pathway, depending on the electronic structure of the unsaturated substrate. Photocatalytic enhancement now appears to be a general phenomenon for hydrophosphination, first reported for zirconium compounds and now applicable to a range of copper compounds. Like zirconium, computational data points to M–P bond weakening as the key contribution of photolysis to reactivity. This improved understanding of copper-based photocatalysis has immediately yielded new reactivity. Most notably, tri-substituted alkenes now appear to be viable substrates for hydrophosphination. All of this reactivity is possible with widely available copper salts that should be the go-to reagents for exploratory hydrophosphination catalysis in synthetic applications, noting that reactivity is easily enhanced with simple irradiation using commercially available light sources. Additionally, this work further demonstrates that study of common laboratory reagents under new conditions can yield new and exciting reactivity. Continued study of this system for expanded substrate scope in hydrophosphination as well as asymmetric hydrophosphination is underway. As more reactivity is identified with specific copper compounds, however, Cu(acac)<sub>2</sub> (**1**) remains the premier catalyst for exploratory hydrophosphination catalysis based on three factors 1) overall activity for the catalyst compared to others for known substrates, 2) accessibility of the catalyst to any synthetic chemist, and 3) reactivity of **1** at ambient temperature under irradiation from a germicidal lamp or even a desk lamp.

## EXPERIMENTAL CONSIDERATIONS

### General Methods

All manipulation of air sensitive compounds were performed under a nitrogen atmosphere with dry, oxygen-free solvents using an M. Braun glovebox or standard Schlenk techniques unless otherwise noted. Compounds **3**,<sup>66</sup> **4**,<sup>67</sup> **7**,<sup>68</sup> **8**,<sup>69</sup> **9**,<sup>54</sup> **12**,<sup>70</sup> and **15**,<sup>70</sup> **16**<sup>71</sup> were synthesized by literature methods. Diphenylphosphine and diphenylphosphine-*d*<sub>1</sub> were synthesized by modified literature procedure by working up with H<sub>2</sub>O or D<sub>2</sub>O, respectively.<sup>37</sup> Chloroform-*d*<sub>1</sub> and benzene-*d*<sub>6</sub> were purchased and then degassed and stored over 3 and 4 Å molecular sieves. Styrene derivatives were distilled or degassed and passed through basic alumina that had previously been dried at 180 °C under reduced pressure. Benzaldehyde was distilled prior to use. All other reagents were acquired from commercial sources and dried by conventional means, as necessary.

ESI-mass spectra were collected on a Waters Xevo G2-XS QTOF high resolution mass spectrometer. All NMR spectra (<sup>1</sup>H, <sup>2</sup>H, <sup>13</sup>C, <sup>31</sup>P, <sup>31</sup>P{<sup>1</sup>H} and <sup>31</sup>P HMB) were recorded at 25 °C with a Bruker AXR 500 MHz or Varian 500 MHz spectrometer. Absorption spectra were recorded with an Agilent Technologies Cary 100 Bio UV-Visible

Spectrophotometer (Santa Clara, CA, USA). EPR data were collected on a Bruker EMXplus EPR spectrometer equipped with an optical cavity. X-ray diffraction data were collected on a Bruker APEX 2 CCD platform diffractometer (Mo Kα (λ = 0.71073 Å)).

**Safety note:** Phosphines are toxic, and many primary phosphines are volatile. Redox reactions or metal catalysts have the potential for rapid hydrogen evolution from phosphine substrates. Appropriate precautions for toxic gases and hydrogen are necessary in this work.

### Additional method for the synthesis of compound 9

In an N<sub>2</sub>-filled glovebox, IPrCuMes<sup>70</sup> (333 mg, 0.583 mmol) was stirred in 5 mL of THF in a scintillation vial. Neat Ph<sub>2</sub>PH (214 mg, 200 μL, 1.15 mmol) was added via micropipette resulting in a yellow solution. The solution was stirred for 16 h at ambient temperature, then volatile materials were removed under reduced pressure to a yellow residue. The crude product was slurried in hexanes, collected on a medium frit, and washed with additional hexanes to afford 278 mg (76%). Spectroscopic data for the product matched that of the literature report.<sup>54</sup>

### General procedure for catalytic experiments

In an N<sub>2</sub>-filled glovebox, 0.019 mmol, 5 mol % of catalyst, 0.38 mmol of unsaturated substrate, and 0.38 mmol of diphenylphosphine or 0.76 mmol of primary phosphine was measured and mixed in 0.6 mL benzene-*d*<sub>6</sub> or chloroform-*d*<sub>1</sub>. This solution was transferred to an NMR tube. Initial <sup>1</sup>H and <sup>31</sup>P{<sup>1</sup>H} NMR spectra were obtained before placing the tube in a photo chamber containing a Rexim G23 UV-A (9W) lamp, Greenlite 23 W CFL bulb, VEI UV Blacklight Party Lamp, or strip of Blue LED lights. Periodic <sup>1</sup>H and <sup>31</sup>P{<sup>1</sup>H} NMR spectra were collected. Conversions were determined by integration of <sup>1</sup>H and <sup>31</sup>P{<sup>1</sup>H} NMR spectra to starting materials. Internal standards varied and included 1,3,5-trimethoxy benzene, tetramethyl silane, or an external standard of PPh<sub>3</sub> (sealed capillary).

### Characterization Data for new phosphines

Previously unreported phosphines were purified by silica gel column chromatography with a 3:1 hexanes: DCM liquid phase in an M. Braun glovebox.

#### 2,4,6-trimethylphenyl(2-phenylpropyl) phosphine (13b):

<sup>1</sup>H NMR (500 MHz, CDCl<sub>3</sub>) δ 7.73 (m, Ar, 2H), 7.22 (m, Ar, 3H), 6.91 (s, Ar, 2H), 4.15 (m, 1H), 2.87 (m, 1H), 2.42 (s, 6H), 2.30 (s, 3H), 1.87 (m, 2H), 1.38 (d, *J* = 6.9 Hz, 3H). <sup>13</sup>C NMR (126 MHz, CDCl<sub>3</sub>) δ 147.12 (s), 141.7 (d, *J* = 11.6 Hz), 137.9 (s), 130.3 (d, *J* = 13.7 Hz), 128.9 (s), 128.4 (s), 126.8 (s), 126.2 (s), 39.3 (d, *J* = 9.8 Hz), 30.4 (d, *J* = 11.1 Hz), 23.6 (d, *J* = 7.1 Hz), 22.9 (d, *J* = 10.9 Hz), 21.0 (s). <sup>31</sup>P{<sup>1</sup>H} NMR (202 MHz, CDCl<sub>3</sub>) δ -93.5 (s). HRMS calcd for C<sub>18</sub>H<sub>23</sub>P: 271.1616 [M+H]<sup>+</sup>, found 271.1615.

**Phenyl(2-methylbutyl)phosphine (13e):** <sup>1</sup>H NMR (500 MHz, CDCl<sub>3</sub>) δ 7.52 (t, *J* = 6.2 Hz, 2H), 7.31 (m, 3H), 4.19 (s, 1H), 1.93 (dd, *J* = 13.6, 5.3 Hz, 1H), 1.73 (m, 1H), 1.50 (dm, *J* = 19.3, 13.4, 6.3 Hz, 2H), 1.27 (m, 1H), 1.00 (d, *J* = 6.6 Hz, 3H), 0.89 (t, *J* = 7.4 Hz, 3H). <sup>13</sup>C NMR (126 MHz, CDCl<sub>3</sub>) δ 136.1 (s), 133.6 (d, *J* = 15.5 Hz), 128.4 (d, *J* = 5.4 Hz), 128.0 (s), 33.5 (d, *J* = 8.5 Hz), 30.9 (d, *J* = 11 Hz), 30.5 (d, *J* = 7.5 Hz), 20.2 (d, *J* = 7.0 Hz), 11.3 (s). <sup>31</sup>P NMR (202 MHz, CDCl<sub>3</sub>) δ -60.5. HRMS calcd for C<sub>11</sub>H<sub>17</sub>P: 181.1146 [M+H]<sup>+</sup>, found 181.1140.

**Cis-2-phenyl-1-phenylphosphino-cyclohexane (13g):** <sup>1</sup>H NMR (500 MHz, CDCl<sub>3</sub>) δ 7.59–6.95 (m, 10H), 3.69 (s, 1H), 3.15 (m, 1H), 2.72 (s, 1H), 2.21 (qd, *J* = 12.5, 3.5 Hz, 1H), 2.04 (m, 1H), 1.98–1.77 (m, 4H), 1.63 (m, 1H), 1.51 (m, 1H). <sup>13</sup>C NMR (126 MHz, CDCl<sub>3</sub>) δ 145.0 (d, *J* = 2.7 Hz), 135.9 (d, *J* = 11.1 Hz), 134.5 (d, *J* = 15.7 Hz), 134.5 (d, *J* = 15.7 Hz), 128.25–128.14 (m), 128.1 (d, *J* = 6.1 Hz), 127.9 (s), 127.7 (d, *J* = 0.9 Hz), 126.2 (s), 46.2 (d, *J* = 11.8 Hz), 41.8 (d, *J* = 11.3 Hz), 30.9 (s), 26.8 (d, *J* = 8.4 Hz), 26.7 (s), 21.5 (d, *J* = 5.3 Hz). <sup>31</sup>P{<sup>1</sup>H} NMR (202 MHz, CDCl<sub>3</sub>) δ -59.1 (s). HRMS calcd for C<sub>18</sub>H<sub>21</sub>P: 269.1459 [M+H]<sup>+</sup>, found 269.1464.

## Computational Methods

All electronic structure calculations were performed on the 380-node IBM Bluemoon cluster at the Vermont Advanced Computing Core with the Gaussian 09 software package.<sup>72</sup> A structural model of **9** was prepared from the molecular structure of **9**<sup>16</sup> determined by X-ray crystallography and optimized using either the generalized gradient approximation (GGA) density functionals PBE<sup>73</sup> or BLYP<sup>74, 75</sup> or the hybrid density functionals PBE0,<sup>73, 76</sup> B3LYP,<sup>74, 75, 77</sup> M06,<sup>78</sup> or M06-L<sup>79</sup> with the def2-TZVP<sup>80</sup> basis set and tight SCF convergence criteria. Geometry optimizations were calculated in solution in tetrahydrofuran, as modelled by a self-consistent reaction field. Avogadro Version 1.2 was used to generate and plot molecular orbitals (MOs). Mulliken orbital populations were obtained with Chemissian Version 4.43 v4.67.<sup>81</sup>

Time-dependent DFT (TDDFT) calculations were performed to assess the MOs involved in the lowest energy transition. TDDFT was used to calculate the first 20 electronic excited states within an expansion space of 100 vectors for each optimized structure using its corresponding density functional. Gausssum<sup>82</sup> was employed to generate TDDFT-predicted absorption spectra by convoluting Gaussian-shaped bands with full width at half-maximum (fwhm) values of 1500 cm<sup>-1</sup>.

## AUTHOR INFORMATION

### Corresponding Author

**Rory Waterman** – Department of Chemistry, University of Vermont, 82 University Pl., Burlington, VT 05405  
orcid.org/0000-0001-8761-8759

E-mail: [rory.waterman@uvm.edu](mailto:rory.waterman@uvm.edu)

### Authors

**Steven Dannenberg** – Department of Chemistry, University of Vermont, 82 University Pl., Burlington, VT 05405  
[orcid.org/0000-0002-3063-7665](https://orcid.org/0000-0002-3063-7665)

**Dennis M. Seth Jr.** – Department of Chemistry, University of Vermont, 82 University Pl., Burlington, VT 05405

**Emma J. Finfer** – Department of Chemistry, University of Vermont 82, University Pl., Burlington, VT 05405

### Notes

The authors declare no competing financial interest.

### ACKNOWLEDGMENT

This research was supported by the U. S. National Science Foundation through CHE-2101766 (to R.W.), a graduate research fellowship for S.G.D. funded by the Vermont Space Grant Consortium under NASA Cooperative Agreement NNX15AP86H and 80NSSC20M0122, and support from the Japan Society for the Promotion of Science (Fellowship to R.W.). EPR measurements were conducted in a spectrometer with optical cavity that was obtained through CHE-1919417 (to R.W.).

## REFERENCES

(1) Iaroshenko, V., *Organophosphorus Chemistry: From Molecules to Applications*. 2019.

- (2) Corbridge, D. E. C., *Phosphorus : chemistry, biochemistry and technology*. 6th ed.; Taylor & Francis: Boca Raton, 2013; p xxxiii, 1439 p.
- (3) Allen, D. W., Phosphines and related C–P bonded compounds. *Organophosphorus Chem.* **2016**, *45*, 1.
- (4) Glueck, D. S., Metal-Catalyzed P–C Bond Formation via P–H Oxidative Addition: Fundamentals and Recent Advances. *J. Org. Chem.* **2020**, *85* (22), 14276–14285.
- (5) Glueck, D. S., Metal-catalyzed nucleophilic carbon–heteroatom (C–X) bond formation: the role of M–X intermediates. *Dalton Trans.* **2008**, 5276.
- (6) Webster, R. L., Beta-Diketiminato Complexes of the First Row Transition Metals: Applications in Catalysis. *Dalton Trans.* **2017**, *46*, 4483.
- (7) Lau, S.; Hood, T. M.; Webster, R. L., Broken Promises? On the Continued Challenges Faced in Catalytic Hydrophosphination. *ACS Catal.* **2022**, 10939–10949.
- (8) Rosenberg, L., Mechanisms of Metal-Catalyzed Hydrophosphination of Alkenes and Alkynes. *ACS Catal.* **2013**, *3* (12), 2845–2855.
- (9) Trifonov, A. A.; Basalov, I. V.; Kissel, A. A., Use of Organolanthanides in the Catalytic Intermolecular Hydrophosphination and Hydroamination of Multiple C–C Bonds. *Dalton Trans.* **2016**, *45*, 19172.
- (10) Sarazin, Y.; Carpentier, J. F., Calcium, Strontium and Barium Homogeneous Catalysts for Fine Chemicals Synthesis. *Chem. Rec.* **2016**, *16*, 2482.
- (11) Seah, J. W. K.; Teo, R. H. X.; Leung, P. H., Organometallic Chemistry and Application of Palladacycles in Asymmetric Hydrophosphination Reactions. *Dalton Trans.* **2021**, *50*, 16909.
- (12) Bange, C. A.; Waterman, R., Challenges in Catalytic Hydrophosphination. *Chem. - Eur. J.* **2016**, *22* (36), 12598.
- (13) Chew, R. J.; Leung, P. H., Our Odyssey with Functionalized Chiral Phosphines: From Optical Resolution to Asymmetric Synthesis to Catalysis. *Chem Rec* **2016**, *16* (1), 141–58.
- (14) Novas, B. T.; Waterman, R., Metal-Catalyzed Hydrophosphination. *ChemCatChem* **2022**, *n/a* (n/a).
- (15) Belli, R. G.; Yang, J.; Bahena, E. N.; McDonald, R.; Rosenberg, L., Mechanism and Catalyst Design in Ru-Catalyzed Alkene Hydrophosphination. *ACS Catal.* **2022**, *12* (9), 5247–5262.
- (16) Horsley Downie, T. M.; Hall, J. W.; Collier Finn, T. P.; Liptrot, D. J.; Lowe, J. P.; Mahon, M. F.; McMullin, C. L.; Whittlesey, M. K., The first ring-expanded NHC–copper(i) phosphides as catalysts in the highly selective hydrophosphination of isocyanates. *Chem. Commun.* **2020**, *56* (87), 13359–13362.
- (17) Lapshin, I. V.; Cherkasov, A. V.; Lyssenko, K. A.; Fukin, G. K.; Trifonov, A. A., N-Heterocyclic Carbene-Coordinated M(II) (M = Yb, Sm, Ca) Bisamides: Expanding the Limits of Intermolecular Alkene Hydrophosphination. *Inorg. Chem.* **2022**, uppo.
- (18) Ji, P.; Sawano, T.; Lin, Z.; Urban, A.; Boures, D.; Lin, W., Cerium-Hydride Secondary Building Units in a Porous Metal–Organic Framework for Catalytic Hydroboration and Hydrophosphination. *J. Am. Chem. Soc.* **2016**, *138*, 14860.
- (19) Espinal-Viguri, M.; King, A. K.; Lowe, J. P.; Mahon, M. F.; Webster, R. L., Hydrophosphination of Unactivated Alkenes and Alkynes Using Iron(II): Catalysis and Mechanistic Insight. *ACS Catal.* **2016**, *6* (11), 7892–7897.
- (20) Varela-Izquierdo, V.; Geer, A. M.; Navarro, J.; López, J. A.; Ciriano, M. A.; Tejel, C., Rhodium Complexes in P–C Bond Formation: Key Role of a Hydrido Ligand. *J. Am. Chem. Soc.* **2021**, *143* (1), 349–358.
- (21) Nolla-Saltiel, R.; Geer, A. M.; Taylor, L. J.; Churchill, O.; Davies, E. S.; Lewis, W.; Blake, A. J.; Kays, D. L.,

- Hydrophosphination of Activated Alkenes by a Cobalt(I) Pincer Complex. *Adv. Synth. Catal.* **2020**, *362*, 3148.
- (22) Barrett, A. N.; Sanderson, H. J.; Mahon, M. F.; Webster, R. L., Hydrophosphination using  $[\text{GeCl}\{\text{N}(\text{SiMe}_3)_2\}_3]$  as a pre-catalyst. *Chem. Commun.* **2020**, *56*, 13623.
- (23) Maiti, R.; Yan, J. L.; Yang, X.; Mondal, B.; Xu, J.; Chai, H.; Jin, Z.; Chi, Y. R., Carbene-Catalyzed Enantioselective Hydrophosphination of  $\alpha$ -Bromoaldehydes to Prepare Phosphine-Containing Chiral Molecules. *Angew. Chem., Int. Ed.* **2021**, *60*, 26616.
- (24) Liu, X. T.; Han, X. Y.; Wu, Y.; Sun, Y. Y.; Gao, L.; Huang, Z.; Zhang, Q. W., Ni-Catalyzed Asymmetric Hydrophosphination of Unactivated Alkynes. *J. Am. Chem. Soc.* **2021**, *143*, 11309.
- (25) Li, Y.-B.; Tian, H.; Yin, L., Copper(I)-Catalyzed Asymmetric 1,4-Conjugate Hydrophosphination of  $\alpha,\beta$ -Unsaturated Amides. *J. Am. Chem. Soc.* **2020**, *142* (47), 20098-20106.
- (26) Yue, W.-J.; Xiao, J.-Z.; Zhang, S.; Yin, L., Rapid Synthesis of Chiral 1,2-Bisphosphine Derivatives through Copper(I)-Catalyzed Asymmetric Conjugate Hydrophosphination. *Angew. Chem. Int. Ed.* **2020**, *59* (18), 7057-7062.
- (27) Ge, L.; Harutyunyan, S. R., Manganese(I)-Catalyzed Access to 1,2-Bisphosphines. *Chem. Sci.* **2022**, *13*, 1307.
- (28) Pérez, J. M.; Postolache, R.; Castiñeira Reis, M.; Sinnema, E. G.; Vargová, D.; de Vries, F.; Otten, E.; Ge, L.; Harutyunyan, S. R., Manganese(I)-Catalyzed H-P Bond Activation via Metal-Ligand Cooperation. *J. Am. Chem. Soc.* **2021**, *143*, 20071.
- (29) Pollard, V. A.; Young, A.; McLellan, R.; Kennedy, A. R.; Tuttle, T.; Mulvey, R. E., Lithium-Aluminate-Catalyzed Hydrophosphination Applications. *Angew. Chem., Int. Ed.* **2019**, *58*, 12291.
- (30) Wang, L.; Yang, F.; Xu, X.; Jiang, J., Organocatalytic 1,6-Hydrophosphination of Para-Quinone Methides: Enantioselective Access to Chiral 3-Phosphoxindoles Bearing Phosphorus-Substituted Quaternary Carbon Stereocenters. *Org. Chem. Front.* **2021**, *8*, 2002.
- (31) Cibazar, M. P.; Dannenberg, S. G.; Waterman, R., A Commercially Available Ruthenium Compound for Catalytic Hydrophosphination. *Isr. J. Chem.* **2020**, *60*, 446.
- (32) Ackley, B. J.; Pagano, J. K.; Waterman, R., Visible-light and thermal driven double hydrophosphination of terminal alkynes using a commercially available iron compound. *Chem. Commun.* **2018**, *54*, 2774.
- (33) Geeson, M. B.; Tanaka, K.; Taakili, R.; Benhida, R.; Cummins, C. C., Photochemical Alkene Hydrophosphination with Bis(trichlorosilyl)phosphine. *J. Am. Chem. Soc.* **2022**, *144* (32), 14452-14457.
- (34) Wang, C.; Huang, K.; Ye, J.; Duan, W.-L., Asymmetric Synthesis of P-Stereogenic Secondary Phosphine-Boranes by an Unsymmetric Bisphosphine Pincer-Nickel Complex. *J. Am. Chem. Soc.* **2021**, *143* (15), 5685-5690.
- (35) Balázs, L. B.; Khalikuzzaman, J. B.; Li, Y.; Csókás, D.; Pullarkat, S. A.; Leung, P. H., Tandem Double Hydrophosphination of  $\alpha,\beta,\gamma,\delta$ -Unsaturated-1,3-Indandiones: Diphosphine Synthesis, Mechanistic Investigations and Coordination Chemistry. *Chem. Commun.* **2019**, *55*, 10936.
- (36) Li, X.-R.; Chen, H. J.; Wang, W.; Ma, M.; Chen, Y.; Li, Y.; Pullarkat, S. A.; Leung, P.-H., Palladacycle promoted asymmetric hydrophosphination of  $\alpha,\beta$ -unsaturated sulfonyl fluorides. *J. Organomet. Chem.* **2019**, *899*, 120912.
- (37) Dannenberg, S. G.; Waterman, R., A bench-stable copper photocatalyst for the rapid hydrophosphination of activated and unactivated alkenes. *Chem. Commun.* **2020**, *56* (91), 14219-14222.
- (38) Lemmen, T. H.; Goeden, G. V.; Huffman, J. C.; Geerts, R. L.; Caulton, K. G., Alcohol elimination chemistry of tetrakis(tert-butoxycopper). *Inorg. Chem.* **1990**, *29* (19), 3680-3685.
- (39) Leyva-Pérez, A.; Vidal-Moya, J. A.; Cabrero-Antonino, J. R.; Al-Deyab, S. S.; Al-Resayes, S. I.; Corma, A., Copper(I)-catalyzed hydrophosphination of styrenes. *J. Organomet. Chem.* **2011**, *696* (1), 362-367.
- (40) Isley, N. A.; Linstadt, R. T. H.; Slack, E. D.; Lipshutz, B. H., Copper-catalyzed hydrophosphinations of styrenes in water at room temperature. *Dalton Trans.* **2014**, *43* (35), 13196-13200.
- (41) Yuan, J.; Zhu, L.; Zhang, J.; Li, J.; Cui, C., Sequential Addition of Phosphine to Alkynes for the Selective Synthesis of 1,2-Diphosphinoethanes under Catalysis. Well-Defined NHC-Copper Phosphides vs in Situ  $\text{CuCl}_2/\text{NHC}$  Catalyst. *Organometallics* **2017**, *36*, 455.
- (42) Chen, Y.-R.; Feng, J.-J.; Duan, W.-L., NHC-copper-catalyzed asymmetric 1,4-addition of diarylphosphines to  $\alpha,\beta$ -unsaturated ketones. *Tetrahedron Lett.* **2014**, *55* (3), 595-597.
- (43) Dannenberg, S. G.; Waterman, R., Cyclo-Tetrakis( $\mu$ -diphenylphosphido)-1,5-bis(tri-tert-butylphosphine)-Tetracopper. *Molbank* **2022**, *2022* (1), M1334.
- (44) Hansch, C.; Leo, A.; Taft, R. W., A survey of Hammett substituent constants and resonance and field parameters. *Chem. Rev.* **1991**, *91* (2), 165-195.
- (45) Lee, D. G.; Congson, L. N., Kinetics and mechanism of the oxidation of alcohols by ruthenate and perruthenate ions. *Can. J. Chem.* **1990**, *68* (10), 1774-1779.
- (46) Kondoh, A.; Yorimitsu, H.; Oshima, K., Copper-Catalyzed anti-Hydrophosphination Reaction of 1-Alkynylphosphines with Diphenylphosphine Providing (Z)-1,2-Diphosphino-1-alkenes. *J. Am. Chem. Soc.* **2007**, *129* (13), 4099-4104.
- (47) Meek, S. J.; Pitman, C. L.; Miller, A. J. M., Deducing Reaction Mechanism: A Guide for Students, Researchers, and Instructors. *J. Chem. Educ.* **2016**, *93* (2), 275-286.
- (48) Heurich, T.; Qu, Z.-W.; Nožinić, S.; Schnakenburg, G.; Matsuoka, H.; Grimme, S.; Schiemann, O.; Streubel, R., Synthesis and Rearrangement of P-Nitroxyl-Substituted PIII and PV Phosphanes: A Combined Experimental and Theoretical Case Study. *Chem. - Eur. J.* **2016**, *22* (29), 10102-10110.
- (49) Kamitani, M.; Itazaki, M.; Tamiya, C.; Nakazawa, H., Regioselective double hydrophosphination of terminal arylacetylenes catalyzed by an iron complex. *J. Am. Chem. Soc.* **2012**, *134* (29), 11932-5.
- (50) Knights, A. W.; Chitnis, S. S.; Manners, I., Photolytic, radical-mediated hydrophosphination: a convenient post-polymerisation modification route to P-di(organo-substituted) polyphosphinoboranes  $[\text{RR}'\text{PBH}_2]_n$ . *Chem. Sci.* **2019**, *10* (30), 7281-7289.
- (51) Staniuk, M.; Zindel, D.; van Beek, W.; Hirsch, O.; Kränzlin, N.; Niederberger, M.; Koziej, D., Matching the organic and inorganic counterparts during nucleation and growth of copper-based nanoparticles – in situ spectroscopic studies. *CrystEngComm* **2015**, *17* (36), 6962-6971.
- (52) Nasibulin, A. G.; Kauppinen, E. I.; Brown, D. P.; Jokiniemi, J. K., Nanoparticle Formation via Copper (II) Acetylacetonate Vapor Decomposition in the Presence of Hydrogen and Water. *J. Phys. Chem. B* **2001**, *105* (45), 11067-11075.
- (53) Widegren, J. A.; Finke, R. G., A review of the problem of distinguishing true homogeneous catalysis from soluble or other metal-particle heterogeneous catalysis under reducing conditions. *J. Mol. Catal. A: Chem.* **2003**, *198* (1), 317-341.
- (54) Fortman, G. C.; Slawin, A. M. Z.; Nolan, S. P., A Versatile Cuprous Synthon:  $[\text{Cu}(\text{IPr})(\text{OH})]$  (IPr = 1,3



- bis(diisopropylphenyl)imidazol-2-ylidene). *Organometallics* **2010**, 29 (17), 3966-3972.
- (55) Zhu, S.; Niljianskul, N.; Buchwald, S. L., Enantio- and Regioselective CuH-Catalyzed Hydroamination of Alkenes. *J. Am. Chem. Soc.* **2013**, 135 (42), 15746-15749.
- (56) Xi, Y.; Hartwig, J. F., Mechanistic Studies of Copper-Catalyzed Asymmetric Hydroboration of Alkenes. *J. Am. Chem. Soc.* **2017**, 139 (36), 12758-12772.
- (57) Scriban, C.; Glueck, D. S.; Zakharov, L. N.; Kassel, W. S.; DiPasquale, A. G.; Golen, J. A.; Rheingold, A. L., P-C and C-C Bond Formation by Michael Addition in Platinum-Catalyzed Hydrophosphination and in the Stoichiometric Reactions of Platinum Phosphido Complexes with Activated Alkenes. *Organometallics* **2006**, 25 (24), 5757-5767.
- (58) Varela-Izquierdo, V.; Geer, A. M.; de Bruin, B.; López, J. A.; Ciriano, M. A.; Tejel, C., Rhodium Complexes in P-H Bond Activation Reactions. *Chem.—Eur. J.* **2019**, 25, 15915.
- (59) Yang, X. Y.; Jia, Y. X.; Tay, W. S.; Li, Y.; Pullarkat, S. A.; Leung, P. H., Mechanistic insights into the role of PC- and PCP-type palladium catalysts in asymmetric hydrophosphination of activated alkenes incorporating potential coordinating heteroatoms. *Dalton Trans.* **2016**, 45, 13449.
- (60) Herron, J. R.; Ball, Z. T., Synthesis and Reactivity of Functionalized Arylcopper Compounds by Transmetalation of Organosilanes. *J. Am. Chem. Soc.* **2008**, 130 (49), 16486-16487.
- (61) Novas, B. T.; Morris, J. A.; Liptak, M. D.; Waterman, R., Effect of Photolysis on Zirconium Amino Phenoxides for the Hydrophosphination of Alkenes: Improving Catalysis. *Photochem* **2022**, 2 (1), 77-87.
- (62) Bange, C. A.; Conger, M. A.; Novas, B. T.; Young, E. R.; Liptak, M. D.; Waterman, R., Light-Driven, Zirconium-Catalyzed Hydrophosphination with Primary Phosphines. *ACS Catal.* **2018**, 8 (7), 6230-6238.
- (63) Kasha, M., Characterization of electronic transitions in complex molecules. *Discuss. Faraday Soc.* **1950**, 9 (0), 14-19.
- (64) Lapshin, I. V.; Yurova, O. S.; Basalov, I. V.; Rad'kov, V. Y.; Musina, E. I.; Cherkasov, A. V.; Fukin, G. K.; Karasik, A. A.; Trifonov, A. A., Amido Ca and Yb(II) Complexes Coordinated by Amidine-Amidopyridinate Ligands for Catalytic Intermolecular Olefin Hydrophosphination. *Inorg. Chem.* **2018**, 57 (5), 2942-2952.
- (65) Garner, M. E.; Parker, B. F.; Hohloch, S.; Bergman, R. G.; Arnold, J., Thorium Metallacycle Facilitates Catalytic Alkyne Hydrophosphination. *J. Am. Chem. Soc.* **2017**, 139 (37), 12935-12938.
- (66) Tambade, P.; Patil, Y.; Nandurkar, N.; Bhanage, B., Copper-Catalyzed, Palladium-Free Carbonylative Sonogashira Coupling Reaction of Aliphatic and Aromatic Alkynes with Iodoaryls. *Synlett* **2008**, 2008, 886-888.
- (67) Chiyindiko, E.; Conrad, J., Redox behaviour of bis( $\beta$ -diketonato)copper(II) complexes. *J. Electroanal. Chem.* **2019**, 837, 76-85.
- (68) Kubas, G. J.; Monzyk, B.; Crumblis, A. L., Tetrakis(Acetonitrile)Copper(I+) Hexafluorophosphate(1-). In *Inorg. Synth.*, 2007; pp 68-70.
- (69) Azoulay, J. D.; Rojas, R. S.; Serrano, A. V.; Ohtaki, H.; Galland, G. B.; Wu, G.; Bazan, G. C., Nickel  $\alpha$ -Keto- $\beta$ -Diimine Initiators for Olefin Polymerization. *Angew. Chem., Int. Ed.* **2009**, 48 (6), 1089-1092.
- (70) Kuehn, L.; Eichhorn, A. F.; Schmidt, D.; Marder, T. B.; Radius, U., NHC-stabilized copper(I) aryl complexes and their transmetalation reaction with aryl halides. *J. Organomet. Chem.* **2020**, 919, 121249.
- (71) Tsuda, T.; Yazawa, T.; Watanabe, K.; Fujii, T.; Saegusa, T., Preparation of thermally stable and soluble mesitylcopper(I) and its application in organic synthesis. *J. Org. Chem.* **1981**, 46 (1), 192-194.
- (72) M. J. Frisch, G. W. T., H. B. Schlegel, G. E. Scuseria, M. A. Robb, J. R. Cheeseman, G. Scalmani, V. Barone, B. Mennucci, G. A. Petersson, H. Nakatsuji, M. Caricato, X. Li, H. P. Hratchian, A. F. Izmaylov, J. Bloino, G. Zheng, J. L. Sonnenberg, M. Hada, M. Ehara, K. Toyota, R. Fukuda, J. Hasegawa, M. Ishida, T. Nakajima, Y. Honda, O. Kitao, H. Nakai, T. Vreven, J. A. Montgomery, Jr., J. E. Peralta, F. Ogliaro, M. Bearpark, J. J. Heyd, E. Brothers, K. N. Kudin, V. N. Staroverov, R. Kobayashi, J. Normand, K. Raghavachari, A. Rendell, J. C. Burant, S. S. Iyengar, J. Tomasi, M. Cossi, N. Rega, J. M. Millam, M. Klene, J. E. Knox, J. B. Cross, V. Bakken, C. Adamo, J. Jaramillo, R. Gomperts, R. E. Stratmann, O. Yazyev, A. J. Austin, R. Cammi, C. Pomelli, J. W. Ochterski, R. L. Martin, K. Morokuma, V. G. Zakrzewski, G. A. Voth, P. Salvador, J. J. Dannenberg, S. Dapprich, A. D. Daniels, Ö. Farkas, J. B. Foresman, J. V. Ortiz, J. Cioslowski, and D. J. Fox, *Gaussian 09*, Wallingford, CT, 2009.
- (73) Perdew, J. P.; Burke, K.; Ernzerhof, M., Generalized Gradient Approximation Made Simple. *Phys. Rev. Lett.* **1996**, 77, 3865.
- (74) Lee, C.; Yang, W.; Parr, R. G., Development of the Colle-Salvetti correlation-energy formula into a functional of the electron density. *Phys. Rev. B: Condens. Matter Mater. Phys.* **1988**, 37 (2), 785.
- (75) Becke, A. D., Density-functional exchange-energy approximation with correct asymptotic behavior. *Phys. Rev. A: At., Mol., Opt. Phys.* **1988**, 38 (6), 3098.
- (76) Perdew, J. P.; Ernzerhof, M.; Burke, K., Rationale for Mixing Exact With Density Functional Approximations. *J. Chem. Phys.* **1996**, 105, 9982.
- (77) Becke, A. D., Density-functional thermochemistry. III. The role of exact exchange. *J. Chem. Phys.* **1993**, 98 (7), 5648.
- (78) Zhao, Y.; Truhlar, D. G., The M06 suite of density functionals for main group thermochemistry, thermochemical kinetics, noncovalent interactions, excited states, and transition elements: two new functionals and systematic testing of four M06-class functionals and 12 other functionals. *Theor. Chem. Acc.* **2008**, 120 (1), 215-241.
- (79) Zhao, Y.; Truhlar, D. G., A new local density functional for main-group thermochemistry, transition metal bonding, thermochemical kinetics, and noncovalent interactions. *J. Chem. Phys.* **2006**, 125 (19), 194101.
- (80) Weigend, F.; Ahlrichs, R., Balanced basis sets of split valence, triple zeta valence and quadruple zeta valence quality for H to Rn: Design and assessment of accuracy. *Phys. Chem. Chem. Phys.* **2005**, 7 (18), 3297.
- (81) Skripnikov, L. Chemissian Version 4.67, Visualization Computer Program. <http://www.chemissian.com>.
- (82) O'Boyle, N. M.; Tenderholt, A. L.; Langner, K. M., cclib: A library for package-independent computational chemistry algorithms. *J. Comput. Chem.* **2008**, 29 (5), 839-845.

